Journal of
Nanomedicine & Nanotechnology

Ashbli and Menzemer, J Nanomed Nanotechnol 2019, 10:2
DOI: 10.35248/2157-7439.19.10.529

Review Article Open Access

On the Fatigue Behavior of Nanocrystalline NiTi Shape Memory Alloys: A Review

Sulaiman Ashbli* and Craig C. Menzemer

Department of Civil Engineering, The University of Akron, Akron, USA

Abstract

This paper presents a review of the research on the fatigue performance of superelastic polycrystalline nanocrystalline NiTi shape memory alloys (nc NiTi SMAs). A brief introduction to some focal definitions and basic concepts of fatigue measurement and response in NiTi SMAs were given. Results found in the literature on fatigue in nc NiTi SMAs are discussed. Mechanical behavior and energy dissipation capacity of nc NiTi SMAs are explored and collectively compared with coarse-grained NiTi SMAs, along with an assessment of the influence of grain size refinement and thermomechanical treatments. Several conclusions and suggestions are made, including that nc NiTi SMAs exhibit larger functional fatigue resistance, lower crack tolerance, higher superelasticity, and smaller hysteresis loss.

Keywords: nc NiTi SMA; Fatigue; Superelasticity; Grain size; Crack growth

Introduction and Background

From seismic dampers to spring tires for future Mars rovers and spacecraft radiators, shape memory alloys are well-established materials in many industries and possess a broad range of functionality and immense application potential [1-3]. SMAs are a type of smart material that possess unique properties including; spontaneous isothermal realignment to the original shape (superelasticity (SE) also referred to as pseudoelasticity), return to the predetermined shape by heating (shape memory effect (SME)), high fatigue strength, vibration absorption, corrosion resistance, and biocompatibility [4-6]. SME was first discovered by Chang and Read in 1951, and later observed by Buehler and Wiley in the near-equiatomic alloy of nickel and titanium (NiTi SMA) or (Nitinol) which stands for NIckel TItanium Naval Ordnance Laboratory [7,8]. NiTi SMAs have two phases; austenite and martensite with three crystallographic structures; twinned martensite, detwinned martensite, and austenite [9]. Furthermore, austenite is a hard material with low ductility, while martensite has a lower yield stress and exhibits more ductile behavior [10]. The high deformation recoverability of SMAs can be attributed in a simplified way to a reversible microscopic solid-solid diffusionless phase transformation between martensite (low-temperature phase) and austenite (high-temperature phase) [11,12] or more specifically between the monoclinic B19′ martensite and the cubic B2 phase austenite [13]. Bain strain and lattice invariant shear (collective shear mechanism) are responsible for producing this atomic rearrangement [14]. Thermal and mechanical stresses are essential for the occurrence of the phase transformation that impacts both SME and SE abilities in these alloys [7]. At high temperatures, cooling NiTi SMA leads to the transformation from the austenite phase to the martensite phase. The transformation initiates at the martensite start temperature (Ms) and is complete at the martensite finish temperature (Mf). Reheating NiTi SMA initiates a reverse transformation that begins at the austenite start temperature (As) and ends at the austenite finish temperature (Af) [15].

The effect of average grain size on materials' strength and fatigue resistance was first described in early 1950s by E. O. Hall and N. J. Petch in iron and steel. Their novel work led to what is known as grain boundary strengthening or Hall-Petch strengthening [16-18]. Nanostructured or nanocrystalline i.e. nc alloys are predominantly assembled of crystallites which represent nano-scale building blocks, while grain boundaries are the adjacent regions between these building blocks [19]. The average grain sizes of typical nc alloys are under 100 nm, and the mechanical properties of alloys are deeply affected by crystallites' chemical composition, atomic structure, and crystallographic orientation [19,20]. Nc NiTi SMAs exhibit superior fatigue resistance with high strain recovery. These properties are best exhibited in SMAs with average grain size below 200 nm and not significantly smaller than 100 nm, where thermally induced martensitic phase transformation is partially suppressed and completely suppressed for average grain sizes smaller than 50 nm [13,21-23].

Nc also known as medical-grade NiTi SMAs generally have average grain sizes below 100 nm, while coarse-grained counterparts have typically an average grain size of 10-100 μm [24-26]. Apart from the direct difference in grain size, the key distinction between nc and coarse-grained NiTi SMAs can be summarized as follows [27,28] (a) the density of the amorphous phase and grain boundary are higher in nc NiTi SMAs, and (b) due to the aforementioned fact the nc NiTi SMAs have number of special qualities including slower heat accumulation in cyclic loading which improves the cyclic stability and the strain recovery rate of the SMAs. Furthermore, nc NiTi SMAs exhibit a broader temperature window for superelasticity and a decrease in deformation rate sensitivity while maintaining good strain recoverability. Shape memory effect can be exhibited by nc NiTi SMAs after thermal treatment which can increase the elastic strain capacity [29].

Nanocrystallization and amorphization (rendering the required nano-scale grains) of coarse-grained NiTi SMA is facilitated using severe plastic deformation (SPD), to reach the required nanocrystalline structure. Recrystallization by heat treatments i.e. annealing needs to succeed one of the following techniques of SPD: high pressure torsion (HPT), cold-rolling, cold-drawing, local canning compression, surface

***Corresponding author:** Sulaiman Ashbli, Department of Civil Engineering, The University of Akron, Akron, USA, Tel: 3307801005; E-mail: sa176@zips.uakron.edu

Received: February 20, 2019; **Accepted:** March 25, 2019; **Published:** April 02, 2019

Citation: Ashbli S, Menzemer CC (2019) On the Fatigue Behavior of Nanocrystalline NiTi Shape Memory Alloys: A Review. J Nanomed Nanotechnol 10: 529. doi: 10.35248/2157-7439.19.10.529

mechanical attrition treatment (SMAT), equal channel angular pressing (ECAP), or accumulative roll bonding (ARB) [27-33]. ECAP of NiTi SMA per se can be utilized to increase yield stress and enhance crack growth resistance [34].

Due to NiTi SMAs high strain recovery rate (~8%), energy dissipation capacity, and biocompatibility; they are employed in many applications of aerospace, civil, robotic, and bioengineering [35,36]. Fatigue is the reason for nearly half of all structural failures in mechanical components [37], and the fact that NiTi SMA structural members in all above-mentioned industries are mostly subjected to cyclic loading makes it difficult to overemphasize the importance of studying the fatigue behavior in these alloys [35]. The significance of lifetime prediction based on fatigue analysis in NiTi SMAs can be highlighted by considering some applications like heart valve and endovascular stents [38]. Unpredictability or the sudden nature of fatigue in NiTi SMAs is one of the main obstacles towards a further increase in Nitinol usage. Although experimental mechanical analysis has been the dominant norm; many techniques have been utilized to model and predict the mechanical behavior of NiTi SMAs based on macro and micro-phenomenological simulation (e.g. finite element), thermodynamics, micromechanics, and molecular dynamics (MD) [39,40].

To date, numerous papers have studied fatigue in NiTi SMAs, but only a handful of them dealt with fatigue in nc NiTi SMAs [22,25,28,31]. Moreover, and to the best of authors' knowledge, none of the previous research provided a review of studies on fatigue in nc Nitinol. Therefore; this paper presents an overview of some basic concepts and definitions of fatigue in NiTi SMAs and delves into its main objective which is exploring research on fatigue in nc Nitinol.

Fatigue of NiTi SMAs

Fatigue types in NiTi SMAs

A material's resistance to repeated cycles of loading is also known as fatigue capacity, which may be categorized into different types based primarily on the characteristics of the material [41]. Fatigue in NiTi SMAs can be attributed to consecutive cycles of thermomechanical phase transformations [42]. As noted by Humbeeck [43], fatigue in NiTi SMAs can be subdivided into three groups; classic (structural) fatigue that ends with the crack propagation failure, thermal cycling fatigue, and degradation (functional) fatigue. Eggeler [44], has further categorized fatigue in NiTi SMAs into two types: functional fatigue and structural fatigue. Functional fatigue or shakedown can be defined as the progressive deterioration of the SE reactivity i.e. functional degradation due to an increase in dislocation density [42,44]. From a stress perspective, functional fatigue transpires if the sum of the residual and applied stress is greater than the critical stress during martensitic transformation [45]. Furthermore, residual strain, change in transformation temperature, and hysteresis or lower dissipated energy all represents symptoms of functional fatigue [42]. Conversely, structural fatigue concerns failure that starting from crack initiation, through crack propagation, and ending with ultimate fracture or separation. The unique chemical composition of NiTi SMAs and their sensitivity to temperature fluctuations [46], impurity level [38], and machining make structural fatigue in NiTi SMAs affected by many thermomechanical and plastic factors along with interaction of martensitic detwinning or stress-induced martensite (SIM) [42,44,47,48].

Structural fatigue in NiTi SMAs

A comprehensive understanding of structural fatigue in NiTi SMAs may not be feasible following conventional fatigue theories directly, partially because of SIM formation that accompanies mechanical deformation [35], and NiTi SMAs are intrinsically phase-oriented materials with unconventional mechanical properties (e.g. large stress plateau (σ_h-σ_l) i.e. maximum stress remains constant for large range of strain) [6,49]. Structural fatigue in NiTi SMAs can be analyzed using a total-life approach (i.e. stress-life fatigue, strain-life fatigue), damage-tolerant analysis, and energy-based methods [50,51]. The total-life approach involves measuring the fatigue crack growth in a specimen that resembles the commercially equivalent structural member (the same heat and surface treatment). The measurement of crack nucleation and propagation depends upon testing the specimen as is, therefore the initial crack emerges from local stress concentration points like surface/subsurface discontinuities or particle/void assemblies (PVA's), inclusions, impurities, and grain boundaries [25,52,53]. On the other hand, the damage-tolerant approach requires introducing a defect into the sample and measuring the crack growth from this defect to analyze fatigue crack propagation [25]. Energy-based methods depend upon finding the relationship between the dissipated energy and the number of cycles to establish a comparison between the superelastic behavior and plastic deformation [54,55].

The NiTi SMAs properties are strongly influenced by the temperature fluctuations; and consequently, mechanical experiments which typically don't include the thermal effects are not sufficient to accurately analyze the fatigue behavior [54]. Moreover, the temperature at which the experimental analyses carried out needs to be comparable to that which the component will be placed i.e. they need to be isothermal (or approximately so). In the case of endodontic rotary NiTi files, it has been shown that the number of cycles to fracture decreases as the temperature increases from room temperature to the actual (*in vivo*) temperature [56]. For small-scale NiTi SMA members like micro-tubes used in endovascular stents, the critical crack size is minuscule and failure quickly follows crack development. Therefore, crack initiation monitoring is recommended instead of crack propagation control [35,57].

Fatigue crack growth and fracture toughness have been studied for thin-walled (400 μm) superelastic nitinol tubes used for endovascular stents, crack paths were monitored using compliance-based methods (capacitance-based load-line displacement gauges), and crack growth behavior, measured in Hanks' balanced saline solution indicated a direct relationship between load ratio and the crack growth [58]. In a study done on 41.3-mm diameter Nitinol rod, the same type of crack monitoring was used, and propagation of crack found to be dependent on temperature and microstructure for all three distinct forms of Nitinol; stable austenite, superelastic austenite, and martensite. Crack growth resistance of both microstructures of austenite found to be similar on the other hand their fatigue crack growth resistance found to be lower than that of martensite [59]. In a study on edge cracked thin sheets of Nitinol (160 μm) the strain fields in the vicinity of the crack has been analyzed using digital image correlation (DIC) [60]. Scanning electron microscopy (SEM) is used to study crack initiation on fracture surface, and to identify stress concentration points [61].

Specimen types and testing methods

Fatigue strength of different NiTi SMAs components can be tested experimentally using four types of specimens [35,38]:

NiTi SMA wires: Used to analyze the fatigue under axial loading, this type of specimens is not suitable for fatigue characterization under torsional and compressive loads.

Surrogate specimens: Resemble the critical properties of actual NiTi SMA member (the same dimensions, identical composition and machining techniques, along with equal thermal and surface treatment as well). Diamond-shaped specimens have been used to replicate the actual components under cyclic bending. Finite element analysis is often used to calculate maximum local strains.

Tension specimens: Dogbone-shaped specimen is commonly used to determine the stress-strain properties of the tested NiTi SMAs. Hollow dogbone-shaped specimens can be used to test fatigue under torsional loading. Specimen alloy composition and thermomechanical history must match those of the finished NiTi SMA member.

Real-life components: Various testing methods used to evaluate fatigue in NiTi SMAs like rotating-bending test or bending rotation fatigue (BRF) (strain-controlled), closed-loop fatigue uniaxial test, closed-loop fatigue multiaxial test, and rotary beam fatigue testing (RBF) (stress-controlled) [35,62]. Fractography is usually carried out using SEM accompanied with energy dispersive X-ray spectroscopy (EDS) to identify the chemical composition and transmission electron microscopy (TEM) to examine formation and growth of dislocations. These techniques are of help to understand the micromechanism of fatigue response [57,62].

Analysis techniques

Fatigue resistance of NiTi SMAs can be assessed using the following methods [25,38,63]:

- Stress-life (S-N) method, using Goodman or Soderberg criteria.
- Strain-life (ε -N) method, was developed by Coffin, Manson, and Morrow.
- Damage-tolerant method, based on fracture mechanics; was first proposed by Paris et al. (Paris law).

As noted in Reference 38, it's essential to confirm that the used strain limit diagrams are not created based on data of two different specimens (e.g. diamond-shaped specimens and tension specimens), since the tensile specimen's data always are more conservative (the whole coupon section will be subjected to the target cyclic strain) than the surrogate specimen data and consequently the strain limit diagram that ensued will not be the same for those two specimens. Using isothermal BRF testing, Rahim et al. [52] studied the low cycle fatigue, and high cycle fatigue of 0.75 mm NiTi wires made of three different SMAs; high purity, maximum allowed level of oxides, and maximum allowed level of carbides alloy. This study showed that surface condition is the most deterministic factor for fatigue resistance in all investigated alloys. The existence of surface defects makes the different alloys experience crack initiation in a similar manner, regardless of their impurity content. It also found that two wires with identical surface treatment can exhibit different fatigue resistance attributable to distinct amounts of PVA's. The amounts of PVA's noted to be of significant effect on crack nucleation as compared to other factors such as embedded particles. Higher oxide contents were observed to be related to larger PVA's and consequently, the wires with maximum oxide level showed the lowest fatigue resistance. On the other hand, cyclic crack propagation appeared to follow the Paris law for all different impurity levels. Fatigue resistance of NiTi SMAs components can be analyzed by applying cyclic loading with zero mean strain. However, in many applications these components are subjected to cyclic loading along with mean or constant strain. Some studies reported that mean strain has a negative impact on fatigue strength [6], while others showed that tensile mean strain had a positive effect on fatigue resistance [64,65]. It has been found that Goodman and Smith-Watson-Topper relationships cannot be applied directly to predict the fatigue behavior since the NiTi SMAs exhibit large plateau regions [6]. Patel suggested employing strain values above and below the SIM for fatigue test in NiTi SMAs as this value is where the reversible martensitic phase transformation occurs [62]. Recent research suggested that fatigue life of NiTi SMAs can be improved by controlling some microstructural features like crystallographic orientation [66]. This paper is by no account intended to provide a review of all studies on fatigue in NiTi SMAs, however, a good account can be found in the following references [35,44,57].

Fatigue in nc NiTi SMA

Grain refinement by SPD has proven to be a feasible way to enhance mechanical properties of NiTi SMA. Pushin et al. showed that SPD followed by annealing of NiTi SMA increased the strain recovery up to 10%, and it was possible for the nc alloy to recover from a stress of 1.5 GPa [67]. Using MD simulation, grain boundaries were found to influence the SME and SE of nc NiTi SMAs. Furthermore, it was shown that pre-training using cyclic loading can reduce the irrecoverable strain that occurs due to plastic deformation at grain boundaries [49]. The increasing number of proposed and existing applications of nc NiTi SMAs in microscopic devices (Microelectromechanical) and stents make fatigue analysis a priority for many recent studies [22,68].

Mechanical fatigue

In a study conducted by Schaffer [22] microcrystalline (mc) NiTi (Ti-50.9 at.% Ni) wires of 177 μm diameter were tested and compared with the same diameter nc NiTi wires. The fatigue capacity of nc NiTi wires at 10^7 cycles found to be 30% larger than their mc NiTi counterparts, moreover, the exhibited isothermal residual strain values of nc NiTi wires were smaller. Rotary beam fatigue at 3600 r/min (60 s^{-1}) in ambient temperature of 24.85^{0}C was used to examine the structural fatigue behavior of five distinct groups of NiTi SMA wires that differ in median grain sizes, with the five selected median grain sizes of: 50 nm, 100 nm, 2 μm, 5 μm, and 10 μm. Strains range varied from 0.5%-1.5% while the maximum number of cycles was 10^8. It was shown that fatigue resistance increases with decreasing grain size. This trend was clearly pronounced for samples with lives between 10^5-10^7 cycles. An alternating strain level of 0.9% was resisted for more than 10^7 cycles by wires with a 50-nm mean grain size while the 10-μm grain wire resisted fracture at strain levels of 0.6% for the same number of cycles.

Resnina et al. [69] studied the effect of grain size on the mechanical properties of Ti-50 at %Ni SMA. Discs of NiTi SMA of 6 mm diameter and 0.1 thickness were used to make bone-shaped samples 5 mm in gage length and a width of 1 mm. After HPT, post-deformation heating was applied. The samples were heated to different temperatures to reach the required median grain sizes (10-550 nm). The studied samples were named after their post-deformation temperature (S359, S365,...). Tension loading and unloading occurred at a rate of 0.01 mm/min on samples at two different temperatures; at 130^{0}C where all samples were in an austenite phase (B2) and at 25^{0}C in which S359 and S365 were in the rhombohedral (R) phase, S380 contained R+ B19′ phases, and S550 was in B19′ phase. It was observed that samples in an austenite B2 phase deformed plastically by dislocation slip without exhibiting SE effect. However, in the samples at 25 ^{0}C, the martensitic reorientation of crystals was observed before slip, which is the same phenomenon found in coarse-grained NiTi SMAs. At 130^{0}C, samples with mean grain sizes of 500 nm exhibited the highest tensile strength and the largest strain values. For samples at 25^{0}C, the highest strength was maintained by samples with a grain size of 40 nm and smaller, while the highest strain values before failure were observed in samples of 500 nm grain size.

A stress-controlled tensile fatigue study of nc NiTi SMA (Ti-53.9 at % Ni) was conducted by Yin et al. [70], using cold-rolled dogbone-shaped samples with final thicknesses of 1.16 mm, gage lengths and widths of 12.5 and 2 mm. 10 nm grain size samples were obtained after cold rolling. However, samples of 42 and 80 nm were obtained after heat treatment. Low-cycle fatigue ($N<10^4$ cycles) tests were performed using a stress of 450 MPa, and intermediate-cycle tests ($N\approx10^4$ cycles) were conducted using a stress of 300 MPa. For a stress level of 300 MPa, the results of the three grain sizes were comparable with an average fatigue life of 15,219 cycles and strain amplitudes of 0.6%, 0.9%, and 1.4%. Stress-strain results of samples tested at 450 MPa and strain amplitudes of 0.9%, 1.6%, and 4.5%, varied significantly based on the median grain size. Fatigue life of 10 nm grain size specimens (6022 cycles) was found to be about three times that of 80 nm sample. An accumulated acoustic energy (AE) technique that utilized the acquisition of acoustic emission signals was evaluated and it was observed that the curves of AE as a function of number of cycles can be divided into three segments. The first two segments included slow and fast crack propagation and could be used to predict fatigue life using AE signals of a sample with an existing crack. It was concluded that the fatigue life of nc NiTi SMAs (other than low-cycle regimen) does not correlate with the hysteresis loop area as their coarse-grained counterparts do. The fatigue life increase for the intermediate-cycle regimen may be attributed to increased concentration of both grain (thickness of about 1 nm acting as elastic frames that constrain crystallite deformation) and phase boundaries (thickness of about 1 nm separates the lattice of austenite from that of martensite). Fracture surface examination of samples can be divided into two groups; the first is micro cracks on surfaces for 10 nm samples under low-cycle fatigue testing conditions as well as all samples subjected to intermediate-cycle fatigue. The second is microvoid dominated surfaces for all low-cycle samples except those with median grain sizes of 10 nm.

In the work carried out by Xiao et al. [71], the fatigue life of Ti-50.2 at.% Ni SMA samples with grain sizes of less than 30 nm was explored using strain-controlled tensile cycling at a frequency of 1 Hz. Cold-rolled dogbone-shaped samples with nominal thicknesses of 0.9 mm and gage lengths and widths of 15 mm and 3 mm respectively, were annealed under conditions to develop grain sizes of 9, 14, 20, and 24 nm. The 6 nm grain size resulted directly after annealing (as rolled). After applying a strain amplitude of 1% and mean strain of 2%, it was noticed that the the degradation of the dissipated energy was lower for samples with grain sizes less than 14 nm. In general, samples with smaller median grain sizes have smaller area encircled by strain-strain curve. The highest fatigue life was measured for 24 nm grain size sample, however, the range of fatigue life for annealed samples was only 238 cycles.

Fatigue crack growth was studied by Le Page et al., using notched (pre-cracked) samples made of Ti-50.9 at % Ni. It was suggested for high ΔK (K_{max}-K_{min}) that samples of 10 nm and 18 nm had lower crack growth rate than other samples in the nanoscale range (42 nm and 80 nm) due to the existence of the residual strain. Positive σ_{xx} and strict crystallographic texture were theorized as reason of the oblique angle of crack growth path for 10 nm samples. It was concluded that samples of 80 nm had the lowest fracture toughness, while 1500 nm samples maintained the highest crack resistance rate. The findings on fracture behavior agree with previously mentioned studies that demonstrated lower fracture toughness for nc NiTi SMAs [72,73]. It has been suggested that conventional coarse-grained materials have lower fatigue resistance if there is no crack. However, the crack growth process advances easier in nc materials due to elevated grain boundary density [72]. Moreover, in a research conducted by Ahadi and Sun on Ti-50.9 at % Ni SMA [73] using rectangular (26 mm × 21 mm) notched compact tension specimens with thicknesses of 1 mm and grain sizes of 10-1500 nm, showed that grain size refinement decreased fracture toughness. Therefore, [72] efforts to increase crack propagation resistance of nc NiTi SMAs represents a promising opportunity to increase the applicability of this type of materials. The granular properties might be customized depending upon requirements for the device being considered. A gradient of grain size might produce some benefits if there was adequate knowledge of the product and all states of loading and environmental conditions.

Thermomechanical fatigue

Many studies explored microstructures made of ultra-fine and nc alloys and showed that their dislocation resistance is higher than that of their coarse-grained counterparts [74,75]. This may interpreted to a certain extent as the smaller the grain size the better the functional performance of the microstructure. Frenzel et al., explored the effect of ultra-fine and nc NiTi SMA on functional fatigue and degradation resistance of spring actuators. Thermomechanical cycling was applied to nc NiTi SMA (Ti-50.1 at %Ni) spring actuators made of 0.8 mm wire. The wire had 20 turns, an outer diameter of 6.5 mm, and grain sizes of 34 nm and 106 nm. The functional behaviour was compared to that of conventional 5.7 µm grain size NiTi SMA actuator. One hundred cycles of heating and cooling were applied to all spring actuators, and a simple mechanism was used to evaluate the thermomechanical response (Figure 1).

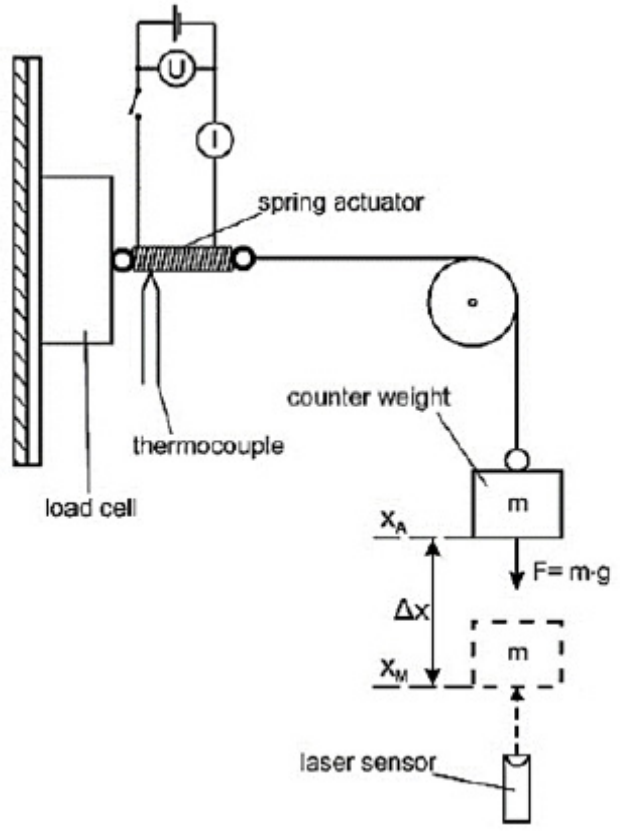

Figure 1: Illustration of the test components in Frenzel et al. study [15].

The heating and cooling cycle used during testing may be explained as follows: the actuator material at low temperature is in a martensite phase and the position of the counterweight as shown in Figure 1 is X_M. Heating the actuator leads to a transformation to austenite which makes the actuator contract which lifts the attached weight. After full contraction X_A is the position and the difference between it and X_M is denoted by ΔX. Cooling the spring actuator results in the reverse transformation to martensite, which the weight returns to X_M. It has been observed that ΔX changes with median grain size; a spring actuator with a grain size of 34 nm had a ΔX equal to 49 mm versus 95 mm for the 5.7 μm grain size actuator. Results from both thermomechanical and differential scanning calorimetry (DSC) cycling showed that grain size refinement is linked with significant improvement in functional fatigue behavior. In the low-temperature state (20^0C), irreversible plastic elongation of 125 mm was recorded for the 5.7 μm grain size actuator after 100 cycles. Conversely, the increase in the 34 nm actuator length was only 15 mm. Accumulation of dislocations leads to a strain buildup, and the number of dislocations is larger in the early stages of cycling. Superior functional stability of nc NiTi SMA actuators was found by Frenzel et al. specifically, grain size refinement introduces a hardening effect which reduces dislocation activity. Furthermore, dislocation initiation is easier in coarse-grained NiTi SMAs and their mobility is higher. Crysallographic homogeneity is better in nc NiTi SMAs due to a lower angle of the B19′ martensite, which leads to smaller accumulated strain. Finally, compound twins found in nc NiTi SMAs have smaller compatibility stresses between them, in contrast with type I and type II twins that exist in conventional NiTi SMAs. It should be noted that extreme grain size refinement is accompanied by several disadvantages, like lower Ms and Mf temperatures that can be lead to incomplete martensitic transformation upon cooling. Therefore, it's essential to optimize the median grain size to obtain a good balance between functionality and stability. It is well known that SME is widely employed in actuators where electrical current is usually used to thermally adjust their shape due to the high-temperature degree for transformation. SE is used generally in medical devices and implants, where the transformation degree is low therefore for these Nitinol alloys the super elastic property is induced by stress, the medical devices and implants are generally in a medium of higher temperature than the transformation degree of SE Nitinol alloy [76,77].

Demers et al. [72] conducted thermomechanical fatigue tests on 1 mm diameter wires made of NiTi SMA (Ti-50.26 at %Ni) subjected to the same post-deformation annealing processes (400^0C for 1 h) in conjunction with water cooling. Five different cold rolling intensities quantified as e = 0.25, 0.75, 1, 1.5, and 2; were used where e provides a measure of work imported to the the material and it is equal to the natural logarithm of the pre-rolling thickness divided by post-rolling thickness ($e = \ln(h_o/h)$). The annealing processes leads to the development of nanograins of (20-120 nm). The reference sample was cold rolled at e=0.25, and annealed at 700^0C for 1 h, followed by water cooling to room temperature. Thermomechanical fatigue capacity was tested using; (a) stress-free recovery, (b) constrained recovery, and (c) assisted two-way SME (ATWSME) (Figure 2.)

Stress-free recovery shows a situation in which the sample approaches the highest value of elastic strain. Constrained recovery is consistent with a case in which the recovery stress is approaches maximum value while the recovery strain is essentially zero. Finally, ATWSME represents a case in which the sample is under axial load and subsequently subjected to heating. The latter process makes the sample contract and lifts the weight due to transformation to an austenite phase. The results of all three techniques utilized by Demers et al. have been used to generate relationships between the recovery stress and recoverable strain. From results obtained for stress-free recovery up to 10^4 cycles or until failure, the following conclusions may be drawn: larger e values were found to be associated with higher recoverable strain (high SE) and a lower strain degradation rate. However, high e values were accompanied by shorter fatigue lives. On the other hand, fatigue life found to be affected by cold rolling intensity; it increased from the reference sample to e = 0.75, but decreased with e values of 1 and larger. The data from constrained recovery for samples with e = 0.25 to 2 for 22×10^4 cycles or failure may be explained as follows: The recovery stress associated with the first cycle found to increase with an increase in e. Cold work increases fatigue life up until e = 0.75. For e = 0.25-2 the correspondent maximum recovery stress values were 550-1200 MPa while the maximum recovery stress for the reference sample was 270 MPa.

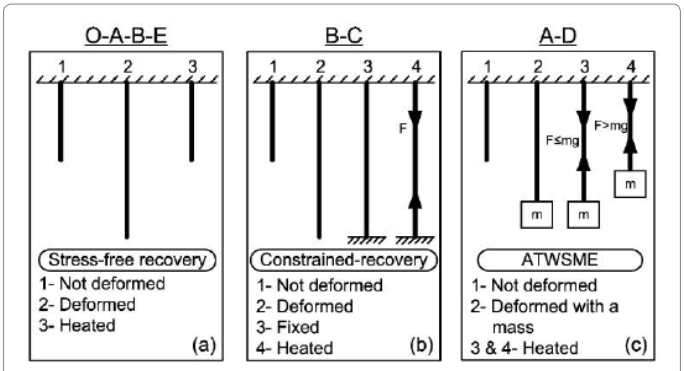

Figure 2: Schematic of test techniques applied by Demers et al. [72].

Specimens of 70 mm length for ATWSME fatigue measurements were tested at a maximum number of cycles of 22×10^4 or up to failure. Recoverable strain values for the same types of samples were plotted with their correspondent number of cycles. It was observed that the reference sample gave the smallest recoverable strain (0.75%) after only two cycles, however, only specimens with e = 0.75-1.5 had lives in excess of 10^4 cycles. Since heating process was carried out up to the temperature in which imposed recoverable strain can be generated, two distinct values of strain are obtained i.e. martensitic and austenitic. The highest value of the strain at the end of the plateau stress obtained when e = 1.5 and e = 2. Various degradation rates were the result of imposing samples to cycling at different levels of controlled recoverable strain. It's conclusively stated that optimum cold rolling for this study was between e = 0.75-2. Furthermore, the cold rolling intensity is inversely proportional to the number of cycles that the sample can withstand. Generally, cold work needs to be applied in order to reach the required nanostructure, and cold work defects are responsible for the low fatigue resistance exhibited by pure nanostructured alloys [78].

The work done by Kreitcberg et al.[79] may be considered complementary to the previous paper. Various types of thermomechanical treatments were carried out on 1 mm diameter wire of NiTi (Ti-50.26 at %Ni) SMA. One of the goals was to explore the properties of NiTi SMA samples that contain nc and amorphous (nanosubgrained (ns)) structures to improve the functional fatigue life associated with nc NiTi SMAs without losing the advantages of the nanostructural components. Introducing an intermediate annealing step (which believed to increase grain and subgrain size and decrease lattice defect density) along with warm rolling resulted in significant enhancement in functional fatigue performance by maintaining both

nc (15-70 nm) and ns structures (about 200 nm). It was concluded that cold rolling (e=1) followed by intermediate annealing (400^{0}C for 1 hr), and finally introducing warm rolling at 150^{0}C (e=0.2), resulted in the sharpest B2-austenite texture which is associated with improved functional fatigue performance (strain recoverability and superelastic response).

Conclusions

The research found in literature on fatigue behavior of nc NiTi SMAs was presented and briefly discussed in this study, the following conclusions can be drawn:

The fatigue response of nc NiTi SMAs studied in the literature generally suggest that as the grain size of samples gets smaller the superelastic properties get better and fracture tolerance gets lower.

Functional fatigue resistance of nc NiTi SMAs are superior to that of coarse-grained NiTi SMAs, however, fatigue crack growth rate seems to be higher for nc NiTi SMAs. The higher crack initiation and dislocation resistance of nc NiTi SMA can be attributed to the effect of high density of grain boundaries.

Deterioration rate of the dissipated energy is lower in nc NiTi and the area surrounded by the strain-stress curve is smaller.

Thermomechanical treatments (cold rolling, warm rolling, intermediate annealing, and post-annealing) can be utilized to enhance nc NiTi fatigue resistance or more specifically crack propagation resistance which can be maintained by obtaining both ns and nc in samples. On the other hand, the AAE technique potentially represents a viable approach to predict fracture resistance capacity.

Introducing standardized techniques to inclusively test nc NiTi SMAs fatigue capacity for both total-life and damage-tolerant approaches would be of benefit in the pursuit of understanding the influence of grain size on fatigue characteristics exhibited by these materials.

There is a need to conduct extensive parametric studies in which fatigue performance can be measured and compared for nc NiTi SMAs that differ in terms of grain size, chemical composition, cycling loading, thermomechanical treatment, and impurities percentage. MD technique represents a promising tool to simulate the fatigue reactivity of nc NiTi SMAs and can be used presumptively to complement the experimental results.

References

1. Bertagne C, Walgren P, Erickson L, Sheth R, Whitcomb J, et al. (2018) Coupled Behavior of Shape Memory Alloy-Based Morphing Spacecraft Radiators: Experimental Assessment and Analysis. Smart Mater Struct.
2. Zhou P, Liu M, Li H, Song G (2018) Experimental Investigations on Seismic Control of Cable-Stayed Bridges Using Shape Memory Alloy Self-Centering Dampers. Struct Control Health Monit p: e2180.
3. https://technology.grc.nasa.gov/patent/LEW-TOPS-99
4. Dolce M, Cardone D (2001) Mechanical Behaviour of Shape Memory Alloys for Seismic Applications 1. Martensite and Austenite NiTi Bars Subjected to Torsion. Int J Mech Sci 43: 2631-2656.
5. Alarcon E, Heller L, Chirani SA, Šittner P, Kopeček J, et al. (2017) Fatigue Performance of Superelastic NiTi near Stress-Induced Martensitic Transformation. Int J Fatigue 95: 76-89.
6. Mahtabi MJ, Shamsaei N, Rutherford B (2015) Mean Strain Effects on the Fatigue Behavior of Superelastic Nitinol Alloys: An Experimental Investigation. Procedia Eng 133: 646-654.
7. Otsuka K, Wayman CM (1999) Shape Memory Materials. Cambridge university press.
8. Jackson CM, Wagner HJ, Wasilewski RJ (1972) 55-Nitinol-the Alloy with a Memory: It's Physical Metallurgy, Properties, and Application: A report. Jena Univ.
9. Leary M, Jani JM, Gibson MA, Subic A (2014) A Review of Shape Memory Alloy Research, Applications and Opportunities.
10. Weafer FM, Bruzzi MS (2016) Micromechanical Investigation into the Effect of Texture on the Fatigue Behaviour of Superelastic Nitinol. Int J Fatigue 93: 148-155.
11. Waitz T, Tsuchiya K, Antretter T, Fischer FD (2009) Phase Transformations of Nanocrystalline Martensitic Materials. MRS Bull 34: 814-821.
12. Peigney M (2018) A Direct Method for Predicting the High-Cycle Fatigue Regime of Shape-Memory Alloys Structures. Advances in Direct Methods for Materials and Structures Springer Pp: 13-28.
13. Waitz T, AntretterT, Fischer FD, Karnthaler HP (2008) Size Effects on Martensitic Phase Transformations in Nanocrystalline NiTi Shape Memory Alloys. Mater Sci Technol 24: 934-940.
14. Bhattacharya K (2003) Microstructure of Martensite: Why It Forms and How It Gives Rise to the Shape-Memory Effect. Oxford University Press.
15. Frenzel J, Burow JA, Payton EJ, Rezanka S, Eggeler G (2011) Improvement of NiTi Shape Memory Actuator Performance Through Ultra-Fine Grained and Nanocrystalline Microstructures. Adv Eng Mater 13: 256-268.
16. Mousavi T, Karimzadeh F, Abbasi MH (2008) Synthesis and Characterization of Nanocrystalline NiTi Intermetallic by Mechanical Alloying. Mater Sci Eng A 487: 46-51.
17. Armstrong RW (2014) 60 Years of Hall-Petch: Past to Present Nano-Scale Connections. Mater Trans 55: 2-12.
18. Li Y, Bushby AJ, Dunstan DJ (2016) The Hall-Petch Effect as a Manifestation of the General Size Effect. Proc R Soc A 472: 20150890.
19. Gleiter H (2000) Nanostructured Materials: Basic Concepts and Microstructure. Acta Mater 48: 1-29.
20. Kumar KS, Van Swygenhoven H, Suresh S (2003) Mechanical Behavior of Nanocrystalline Metals and Alloys1. Acta Mater 51: 5743-5774.
21. Waitz T, Kazykhanov V, Karnthaler HP (2004) Martensitic Phase Transformations in Nanocrystalline NiTi Studied by TEM. Acta Mater 52: 137-147.
22. Schaffer JE (2009) Structure-Property Relationships in Conventional and Nanocrystalline NiTi Intermetallic Alloy Wire. J Mater Eng Perform 18: 582-587.
23. Paul PP, Paranjape HM, Amin-Ahmadi B, Stebner AP, Dunand DC, et al. (2017) Effect of Machined Feature Size Relative to the Microstructural Size on the Superelastic Performance in Polycrystalline NiTi Shape Memory Alloys. Mater Sci Eng A 706: 227-235.
24. Hanlon T, Tabachnikova ED, Suresh S (2005) Fatigue Behavior of Nanocrystalline Metals and Alloys. Int J Fatigue 27: 1147-1158.
25. Robertson SW, Pelton AR, Ritchie RO (2012) Mechanical Fatigue and Fracture of Nitinol. Int Mater Rev 57: 1-37.
26. Xu D (2012) Characterization of in Situ Deformation Texture in Superelastic Nitinol. PhD Thesis UC Berkeley.
27. Ahadi A, Sun Q (2014) Effects of Grain Size on the Rate-Dependent Thermomechanical Responses of Nanostructured Superelastic NiTi. Acta Mater 76: 186-197.
28. Xia M, Sun Q (2017) Grain Size Effects on Stability of Nonlinear Vibration with Nanocrystalline NiTi Shape Memory Alloy. Smart Mater Struct 26: 105033.
29. Belyaev S, Resnina N, Pilyugin V, Glazova D, Zeldovich V, et al. (2017) Shape Memory Effects in Ti-50.2 At% Ni Alloy with Different Grain Size. Mater Sci Eng A 706: 64-70.
30. Sanusi KO, Akinlabi ET, Mwita WW (2017) Accumulative Roll Bonding (ARB) Process for Effective Biomedical NiTi Alloys. ASME 2017 International Mechanical Engineering Congress and Exposition, American Society of Mechanical Engineers, p: V003T04A059-V003T04A059.
31. Arunkumar S, Kumaravel P, Velmurugan C, Senthilkumar V (2018) Microstructures and Mechanical Properties of Nanocrystalline NiTi Intermetallics Formed by Mechanosynthesis. Int J Miner Metall Mater 25: 80-87.
32. Sergueeva AV, Song C, Valiev RZ, Mukherjee AK (2003) Structure and Properties of Amorphous and Nanocrystalline NiTi Prepared by Severe Plastic Deformation and Annealing. Mater Sci Eng A 339: 159-165.

33. Mei QS, Zhang L, Tsuchiya K, Gao H, Ohmura T, et al. (2010) Grain Size Dependence of the Elastic Modulus in Nanostructured NiTi. Scr Mater 63: 977-980.

34. Leitner T, Sabirov I, Pippan R, Hohenwarter A (2017) The Effect of Severe Grain Refinement on the Damage Tolerance of a Superelastic NiTi Shape Memory Alloy. J Mech Behav Biomed Mater 71: 337-348.

35. Mahtabi MJ, Shamsaei N, Mitchell MR (2015) Fatigue of Nitinol: The State-of-the-Art and Ongoing Challenges. J Mech Behav Biomed Mater 50: 228-254.

36. Van Humbeeck J (1999) Non-Medical Applications of Shape Memory Alloys. Mater Sci Eng A 273: 134-148.

37. Stephens RI, Fatemi A, Stephens RR, Fuchs HO (2000) Metal Fatigue in Engineering. John Wiley & Sons.

38. Bonsignore C (2017) Present and Future Approaches to Lifetime Prediction of Superelastic Nitinol. Theor Appl Fract Mech 92: 298-305.

39. Chowdhury P (2018) Frontiers of Theoretical Research on Shape Memory Alloys: A General Overview. Shape Mem Superelasticity Pp: 1-15.

40. Li MP, Sun QP (2018) Nanoscale Phase Transition Behavior of Shape Memory Alloys-Closed Form Solution of 1D Effective Modelling. J Mech Phys Solids 110: 21-37.

41. Wood WA (1972) Four Basic Types of Metal Fatigue. george washington univ washington dc inst for the study of fatigue fracture and structural reliability.

42. LePage WS, Ahadi A, Lenthe WC, Sun QP, et al. (2018) Grain Size Effects on NiTi Shape Memory Alloy Fatigue Crack Growth. J Mater Res 33: 91-107.

43. Van Humbeeck J (1991) Cycling Effects, Fatigue and Degradation of Shape Memory Alloys. J Phys IV 1: C4-189.

44. Eggeler G, Hornbogen E, Yawny A, Heckmann A, Wagner M (2004) Structural and Functional Fatigue of NiTi Shape Memory Alloys. Mater Sci Eng A 378: 24-33.

45. Gao Y, Casalena L, Bowers ML, Noebe RD, Mills MJ, et al. (2017) An Origin of Functional Fatigue of Shape Memory Alloys. Acta Mater 126: 389-400.

46. Dosanjh A, Paurazas S, Askar M (2017) The Effect of Temperature on Cyclic Fatigue of Nickel-Titanium Rotary Endodontic Instruments. J Endod 43: 823-826.

47. Mahtabi MJ, Shamsaei N (2017) Fatigue Modeling for Superelastic NiTi Considering Cyclic Deformation and Load Ratio Effects. Shape Mem Superelasticity 3: 250-263.

48. Rao A, Srinivasa AR (2018) A Thermodynamic Driving Force Approach for Analyzing Functional Degradation of Shape Memory Alloy Components. Mech Adv Mater Struct Pp: 1-13.

49. Ko WS, Maisel SB, Grabowski B, Jeon JB, Neugebauer J (2017) Atomic Scale Processes of Phase Transformations in Nanocrystalline NiTi Shape-Memory Alloys. Acta Mater 123: 90-101.

50. Pelton AR (2011) Nitinol Fatigue: A Review of Microstructures and Mechanisms. J Mater Eng Perform 20: 613-617.

51. Moumni Z, Van Herpen A, Riberty P (2005) Fatigue Analysis of Shape Memory Alloys: Energy Approach. Smart Mater Struct 14: S287.

52. Rahim M, Frenzel J, Frotscher M, Pfetzing-Micklich J, Steegmüller R, et al. (2013) Impurity Levels and Fatigue Lives of Pseudoelastic NiTi Shape Memory Alloys. Acta Mater 61: 3667-3686.

53. Bagheri A, Mahtabi MJ, Shamsaei N (2018) Fatigue Behavior and Cyclic Deformation of Additive Manufactured NiTi. J Mater Process Technol 252: 440-453.

54. Rao A, Srinivasa AR, Reddy JN (2015) Design of Shape Memory Alloy (SMA) Actuators. Springer.

55. Zhang Y, Zhu J, Moumni Z, Van Herpen A, Zhang W (2016) Energy-Based Fatigue Model for Shape Memory Alloys Including Thermomechanical Coupling. Smart Mater Struct 25: 035042.

56. Dosanjh A, Paurazas S, Askar M (2017) The Effect of Temperature on Cyclic Fatigue of Nickel-Titanium Rotary Endodontic Instruments. J Endod 43: 823-826.

57. Kang G, Song D (2015) Review on Structural Fatigue of NiTi Shape Memory Alloys: Pure Mechanical and Thermo-Mechanical Ones. Theor Appl Mech Lett 5: 245-254.

58. Robertson SW, Ritchie RO (2007) In Vitro Fatigue-Crack Growth and Fracture Toughness Behavior of Thin-Walled Superelastic Nitinol Tube for Endovascular Stents: A Basis for Defining the Effect of Crack-like Defects. Biomaterials 28: 700-709.

59. McKelvey A, Ritchie R (2001) Fatigue-Crack Growth Behavior in the Superelastic and Shape-Memory Alloy Nitinol. Metall Mater Trans A 32: 731-743.

60. Daly S, Miller A, Ravichandran G, Bhattacharya K (2007) An Experimental Investigation of Crack Initiation in Thin Sheets of Nitinol. Acta Mater 55: 6322-6330.

61. Maletta C, Sgambitterra E, Furgiuele F, Casati R, Tuissi A (2014) Fatigue Properties of a Pseudoelastic NiTi Alloy: Strain Ratcheting and Hysteresis under Cyclic Tensile Loading. Int J Fatigue 66: 78-85.

62. Patel MM (2007) Characterizing Fatigue Response of Nickel-Titanium Alloys by Rotary Beam Testing. J ASTM Int 4: 1-11.

63. Paris P, Erdogan F (1963) A Critical Analysis of Crack Propagation Laws. J Basic Eng 85: 528-533.

64. Morgan NB, Painter J, Moffat A (2004) Mean Strain Effects and Microstructural Observations during in Vitro Fatigue Testing of NiTi. Proceedings of the International Conference on Shape Memory and Superelastic Technologies. Pacific Grove, CA: SMST Society Pp: 303-310.

65. Pelton AR, Schroeder V, Mitchell MR, Gong XY, Barney M, et al. (2008) Fatigue and Durability of Nitinol Stents. J Mech Behav Biomed Mater 1: 153-164.

66. Paul PP, Fortman M, Paranjape HM, Anderson PM, Stebner AP, et al. (2018) Influence of Structure and Microstructure on Deformation Localization and Crack Growth in NiTi Shape Memory Alloys. Shape Mem Superelasticity Pp: 1-9.

67. Pushin VG, Stolyarov VV, Valiev RZ, Lowe TC, Zhu YT (2005) Nanostructured TiNi-Based Shape Memory Alloys Processed by Severe Plastic Deformation. Mater Sci Eng A 410: 386-389.

68. San Juan J, Nó ML, Schuh CA (2009) Nanoscale Shape-Memory Alloys for Ultrahigh Mechanical Damping. Nat Nanotechnol 4: 415.

69. Resnina N, Belyaev S, Pilugin V, Glazova D (2017) Mechanical Behavior of Nanostructured TiNi Shape Memory Alloy with Different Grain Size. Mater Today Proc 4: 4841-4845.

70. Yin H, He Y, Moumni Z, Sun Q (2016) Effects of Grain Size on Tensile Fatigue Life of Nanostructured NiTi Shape Memory Alloy. Int J Fatigue 88: 166-177.

71. Xiao Y, Zeng P, Lei L (2017) Grain Size Effect on Mechanical Performance of Nanostructured Superelastic NiTi Alloy. Mater Res Express 4: 035702.

72. Demers V, Brailovski V, Prokoshkin SD, Inaekyan KE (2009) Thermomechanical Fatigue of Nanostructured Ti-Ni Shape Memory Alloys. Mater Sci Eng A 513: 185-196.

73. Ahadi A, Sun Q (2016) Grain Size Dependence of Fracture Toughness and Crack-Growth Resistance of Superelastic NiTi. Scr Mater 113: 171-175.

74. Qian T, Marx M, Schüler K, Hockauf M, Vehoff H (2010) Plastic Deformation Mechanism of Ultra-Fine-Grained AA6063 Processed by Equal-Channel Angular Pressing. Acta Mater 58: 2112-2123.

75. Huang CX, Yang G, Gao YL, Wu SD, Zhang ZF (2008) Influence of Processing Temperature on the Microstructures and Tensile Properties of 304L Stainless Steel by ECAP. Mater Sci Eng A 485: 643-650.

76. Barrett PR, Fridline D (2002) User Implemented Nitinol Material Model in ANSYS. Pp: 1-6.

77. Mizar SP (2005) Thermomechanical Characterization of NiTiNOL and NiTiNOL Based Structures Using ACES Methodology.

78. Prokoshkin S, Brailovski V, Inaekyan K, Korotitskiy A, Kreitcberg A (2015) Thermomechanical Treatment of TiNi Intermetallic-Based Shape Memory Alloys. Mater Sci Found.

79. Kreitcberg A, Brailovski V, Prokoshkin S, Facchinello Y, Inaekyan K, et al. (2013) Microstructure and Functional Fatigue of Nanostructured Ti-50.26 At% Ni Alloy after Thermomechanical Treatment with Warm Rolling and Intermediate Annealing. Mater Sci Eng A 562: 118-127.